International Journal of Biological Macromolecules 288 (2025) 138693

Contents lists available at ScienceDirect

International Journal of Biological Macromolecules

journal homepage: www.elsevier.com/locate/ijbiomac

Injectable cell-laden gelatin-chondroitin sulphate hydrogels for liver *in vitro* models

E. Sanchez-Gonzalez [a,b], R. Naranjo-Alcazar [a], I. Tort-Ausina [a,b], M.T. Donato [c,d,e], M. Salmeron-Sanchez [a,b,f], L. Tolosa [b,c,*], G. Gallego-Ferrer [a,b,**]

[a] Center for Biomaterials and Tissue Engineering (CBIT), Universitat Politècnica de València, Valencia 46022, Spain
[b] Biomedical Research Networking Centre on Bioengineering, Biomaterials and Nanomedicine (CIBER-BBN), Carlos III Health Institute, Valencia 46022, Spain
[c] Experimental Hepatology Unit, Health Research Institute La Fe (IISLAFE), Valencia 46026, Spain
[d] Faculty of Medicine, Department of Biochemistry and Molecular Biology, University of Valencia, Valencia 46010, Spain
[e] Biomedical Research Networking Center in Hepatic and Digestive Diseases (CIBERehd), Carlos III Health Institute, 28029 Madrid, Spain
[f] Centre for the Cellular Microenvironment, University of Glasgow, G12 8LT Glasgow, United Kingdom

ARTICLE INFO

Keywords:
Hydrogel
Gelatin
Chondroitin sulphate
HepG2 cells
Functionality
3D culture

ABSTRACT

Liver extracellular matrix-based models that precisely reproduce liver physiology and functions are required as 3D culture microenvironments for multiple applications in toxicology and metabolism, or for understanding the mechanisms implicated in liver disease. We introduced injectable gelatin-chondroitin sulphate (Gel/CS) hydrogels for culturing HepG2 cells, and evaluated the mechanical properties and functionality of cells in different Gel/CS compositions. The Gel/CS hydrogels exhibited soft mechanical properties and allowed the HepG2 culture. The characterisation and comparison of 3D cultures to standard monolayer systems revealed the regulation of key hepatic markers (*i.e. CYP3A4*, *GSTA1*) when cells were cultured in the Gel/CS hydrogels compared to 2D cultures, and also enhanced urea and albumin production, which would indicate increased cells functionality. This study underpins 3D *in vitro* models based on the Gel/CS hydrogels that can be used for different hepatology applications by offering increased predictivity and physiological relevance compared to current *in vitro* models.

1. Introduction

The liver is a vital organ whose major functions include metabolic regulation, detoxification, immune functions and synthesis of vital proteins like albumin [1]. The liver is composed of various cell types. Hepatocytes are the main cell type, perform the majority of hepatic functions and account for approximately 80 % of the liver cell mass. Additionally, there are non-parenchymal cells (Kupffer cells, hepatic stellate cells and sinusoidal endothelial cells) that ensure proper liver functioning [2].

Liver *in vitro* models attempt to mimic liver functions to provide insights into drug metabolism and toxicity, or for understanding the mechanisms implicated in liver diseases, by reducing the need for animal testing. Presently, the "gold standard" *in vitro* model is the two-dimensional (2D) culture of primary human hepatocytes (PHHs) [3,4]. However, PHHs cultured in 2D dedifferentiate within hours and lose their polarity and key functions, such as albumin production or cytochrome P450 (CYP) activity, which leads to limited predictive models [4,5]. To improve the performance of classic *in vitro* models, three-dimensional (3D) manufacturing techniques have been introduced to mimic the spatial arrangement of cells and interactions with the extracellular microenvironment, including the liver extracellular matrix (ECM) [6].

Liver cells are functionally organised in the ECM, which is composed mainly of collagen type I in combination with proteoglycans and glycosaminoglycans, such as hyaluronic acid or chondroitin sulphate (CS) [1,2,7]. Of the different proposed 3D systems, hydrogels offer a highly hydrated environment like native tissue, fast gelation times and tunable

* Correspondence to: L. Tolosa, Experimental Hepatology Unit, Health Research Institute La Fe (IISLAFE), Av Fernando Abril Martorell 106, 46026, Valencia, Spain.
** Correspondence to: G. Gallego-Ferrer, Center for Biomaterials and Tissue Engineering (CBIT), Universitat Politècnica de València, Camino de vera s/n, 46022, Valencia, Spain.
E-mail addresses: laiatolosa@hotmail.com (L. Tolosa), ggallego@ter.upv.es (G. Gallego-Ferrer).

https://doi.org/10.1016/j.ijbiomac.2024.138693
Received 11 March 2024; Received in revised form 7 December 2024; Accepted 10 December 2024
Available online 12 December 2024

viscoelastic properties, which allow them to be scalable for bioprinting techniques if they are injectable, and to ensure homogeneous cell encapsulation [8,9].

In an attempt to mimic the liver ECM, gelatin (Gel) has been used as an alternative to collagen because it avoids the disadvantages linked with complex handling and the high cost of collagen [10]. Moreover, Gel promotes cell-adhesion through the Arg-Gly-Asp (RGD) sequence [11,12], and the hepatic cells encapsulated in Gel have shown increased expression of cytochromes and albumin and urea production compared to 2D [13,14]. Previously, our group showed that the Gel and hyaluronic acid combination for the culture of liver cells resulted in improved functionality of both HepG2 cells and PHHs [15]. CS has been involved in several important biological functions, such as proliferation, inflammation or tissue repair [16] and has been also described to play a role in liver disease [17]. The combination of Gel hydrogels with glycosaminoglycans like CS for liver *in vitro* studies has not been profoundly explored. Hence, we studied the effect of CS on the physico-chemical properties of tyramined Gel/CS hydrogels and its biological impact on encapsulated liver cells.

2. Materials and methods

2.1. Materials

Gel from porcine skin (gel strength 300, Type A), chondroitin sulphate (sodium salt) from shark cartilage, tyramine hydrochloride, sodium chloride, 2-(N-Morpholino)ethanesulfonic acid (MES), N-Hydroxysuccinimide (NHS), horseradish peroxidase (HRP), hydrogen peroxide (H_2O_2, 30 %, *w*/w in water), bovine serum albumin (BSA), ammonium chloride (NH_4Cl), saline HEPES and TRI Reagent® were acquired from Sigma-Aldrich (St. Louis, USA). Real-time reverse transcription polymerase chain reaction (RT-PCR) reagents and the SYBR Green I Master PCR Mix were bought from InvitrogenTM (Carlsbad, USA). N-(3-Dimethylaminopropyl)-N′-ethylcarbodiimide (EDC) was obtained from Iris Biotech GmbH (Marktredwitz, Germany). Dialysis membranes were purchased from Thermo Fisher (Massachusetts, USA). The materials used in the cell culture were purchased from GIBCO (Gibco BRL, Paisley, UK), and Matrigel® came from Corning (NY, USA).

2.2. Synthesis of tyramined Gel/CS hydrogels

Gel and CS tyramined conjugates (Gel-Tyr and CS-Tyr) were prepared according to the procedure reported by Sakai S. et al. [18] and Zhang, Y. et al. [19], respectively. The degree of tyramine substitution for the Gel-Tyr and CS-Tyr conjugates was calculated as in [20]. The molecular weight of the pristine and modified Gel and CS were measured by gel permeation chromatography [21]. Hydrogels (4 %, *w/v*) were synthesised by enzymatic crosslinking at different Gel-Tyr to CS-Tyr (Gel/CS) volume ratios: 100/0, 75/25, 50/50, 25/75 and 0/100. Horseradish peroxide and hydrogen peroxide (H_2O_2), at a final concentration in hydrogel of 1.25 U/mL and 2 mM, respectively, were used as catalysers of the crosslinking reaction [15]. Lyophilised powders of Gel-Tyr and CS-Tyr were dissolved in F12 media. Gel-Tyr solution (4 %, *w/v*) was prepared at 37 °C for 1–2 h and CS-Tyr (4 %, w/v) solution was made at 3 °C for 2–3 h. Hydrogels were prepared with 80 %, *v*/v, Gel/CS, 10 %, v/v, HRP and 10 %, v/v, H_2O_2 solutions. The HRP aliquot was mixed with Gel/CS solution and placed on a surface (or inside a mould). Then hydrogels were formed by dropping the H_2O_2 aliquot.

2.3. Physico-chemical characterisation of the gel/CS hydrogels

Mechanical properties were measured on the hydrogels swollen in HepG2 culture media for 24 h using a rheometer (DHR, TA Instruments, New Castle, USA). The linear viscoelastic region was determined by a dynamic strain sweep test at a frequency of 1 Hz. A dynamic frequency sweep test was performed in the linear viscoelastic region at 1 % strain to obtain the storage modulus (G') and the loss modulus (G'') of hydrogels. Gelation time was determined by dynamic time sweep at 1 Hz frequency and 1 % strain on the hydrogels crosslinked on the rheometer plates [22]. Glass transition temperatures (T_g) were determined with a differential scanning calorimeter (Mettler Toledo DSC, Ohio, USA) at a scan rate of 10 °C/min within the temperature 130–50 °C range in a nitrogen flow of 60 mL/min. Prior to measurements, hydrogels were placed inside a desiccator with 75 % relative humidity for 7 days. With equilibrium water content, obtained following the procedure reported by Sanmartin-Masia et al. [21], the crosslinking density [15] and the modulus of the dry hydrogels were calculated using a simplified version of the rubber elasticity theory [15,23]. For the morphological characterisation by field emission scanning electron microscopy (FE-SEM) (Ultra 55, Zeiss), hydrogels were lyophilised and cut into sections, which were platinum-covered before observations. Photo acquisition was performed at an acceleration voltage of 2 kV and images were analysed using the ImageJ software (National Institutes of Health, US) to obtain the mean pore size.

2.4. Cell culture

HepG2 cells (ECACC No. 85011430) were cultured in Ham's F12/Leibovitz L15 (1:1, *v*/v) supplemented with 5 % foetal bovine serum, L-glutamine (3.5 mM), BSA (2 mg/mL), glucose (5 mM), bicarbonate (12 mM) and 1 % penicillin/streptomycin. For subculturing purposes, cells were treated with 0.25 % trypsin/0.02 % EDTA at 37 °C to detach them and were seeded at a density of 1×10^5 cells/cm^2. Cells were cultured at 37 °C and 5 % CO_2 in an incubator.

HepG2 cells were encapsulated in the hydrogels of Gel/CS compositions 100/0, 75/25 and 50/50 to test the cell response on the proposed platform. Hydrogels were synthesised following the procedure written in Section 2.2. Cells were resuspended in precursor polymer solutions, previously sterilised by filtering, and encapsulated in 100 μL hydrogels in a 48-well plate at a final concentration of 2×10^6 cells/mL (in hydrogel). After 20 min this allowed to enable complete gelation, and fresh medium was added and well plates were incubated. As controls, the cells seeded at the same density in the monolayer (the 2D control) and also the cells encapsulated in the 3D commercial matrix Matrigel® (3D control) were used. The medium was refreshed every day. Viability, functional and gene expression analyses were performed after 1, 3 and 5 days.

2.5. Cell viability assessment

Biocompatibility was tested by incubating cell cultures with propidium iodide (PI, 1.5 μL/mL) and Hoechst 33342 (Hoe, 1.5 μL/mL) for 30 min at 37 °C. After incubation, cells were imaged under a Leica HMR microscope (Leica Microsystems, Wetzlar, Germany). Viability was calculated after quantifying live and dead cells with ImageJ (National Institutes of Health, USA).

2.6. Immunofluorescence

Samples were prepared for confocal microscopy as previously described in detail by Rodriguez-Fernandez et al. [15]. In this study, sections were incubated with the corresponding primary and secondary antibodies (Supplementary Table S1). Controls were performed with no primary antibody to check non-specific reactions, and no fluorescence was detected. Immunofluorescence images were acquired with a Leica DMI8 confocal microscope and the LASX software (Leica, USA) was used for image processing.

2.7. Determination of urea and albumin production

Urea was quantified with the QuantinChrom™ Urea Assay kit (BioAssays, Hayward, CA, USA) and albumin with the Human Albumin

ELISA kit (Bethyl Laboratories, Montgomery, TX, USA). All the results were calculated by following the manufacturer's instructions and normalised by RNA values.

2.8. Transcriptomic characterisation of the key hepatic markers

Samples were mechanically disaggregated with a homogeniser (Ultraturrax). Trizol lysis reagent and chloroform were added at the 5:1 ratio, and total RNA was extracted by the RNeasy Plus Micro kit (Qiagen, Madrid, Spain) following the manufacturer's instructions. RNA was reverse-transcribed and real-time-quantified using the appropriate primers (Supplementary Table S2) as previously described by Moya et al. [24]. The relative mRNA expression was calculated by the method described by Vandesompele et al. [25,26]. The relative mRNA expression was expressed as fold change compared to the monolayer cultures and normalised using human housekeeping *GAPDH* and *RPLP0* genes. A reference calibrator cDNA was included.

2.9. Statistical analysis

The results are provided as the mean ± standard deviation (SD). Experiments were performed by triplicates, except for albumin quantification, which was done by duplicates. The Student's *t*-test was run to make a comparison between two groups. For multiple comparisons, the statistical significance of the mean differences was evaluated by One-way ANOVA and Tukey's multiple comparisons post-test. $P < 0.05$ was assumed statistically significant and calculated using GraphPad Prism v9 (San Diego, CA, USA).

3. Results

3.1. Enzymatically crosslinked gel/CS hydrogels

Gel and CS were chemically modified by tyramine grafting to enzymatically crosslink them with HRP and H_2O_2, and to form hydrogels, as previously described in Poveda-Reyes et al. [27] and Nguyten et al. [28] (Fig. 1A). Gel and CS had a tyramine substitution degree of 1.95×10^{-7} molTyr/mg and 2.57×10^{-7} molTyr/mg, respectively, (Supplementary Fig. S1).

The tyramine conjugates presented a lower molecular weight (Mw) than the unmodified ones. Pristine Gel and Gel-Tyr exhibited an Mw value of 57 ± 6 kDa and 15 ± 4 kDa, respectively. Pristine CS had an Mw of 106 ± 11 kDa and a CS-Tyr of 98 ± 7 kDa. All the hydrogel mixtures were successfully synthesised in F12 medium (Fig. 1B). No signs of macroscopic phase separation were visible in mixtures, which could indicate the homogeneity of hydrogel components. The gelation times of the different hydrogels, obtained from the crosslinking kinetics (Fig. 1C), are listed in Table 1.

Gelation time varied between 2 min and 5 min, and was longer for the CS-enriched mixtures as previously described [19,29]. All the hydrogels presented an interconnected honeycomb-like porous structure (Fig. 2), as typically described by different authors for the Gel [21] and CS [19,28] hydrogels. However, differences between compositions were observed (Fig. 2) because pore size considerably increased in the compositions with CS (Table 1). Despite the difference in crosslinking time, no phase separation between Gel and CS in the hydrogel mixtures was observed when samples were observed by FE-SEM (Fig. 2), which may be explained by the same crosslinking mechanism. Fig. 2F shows the heating curves (2nd scan) obtained on all the equilibrated hydrogels at

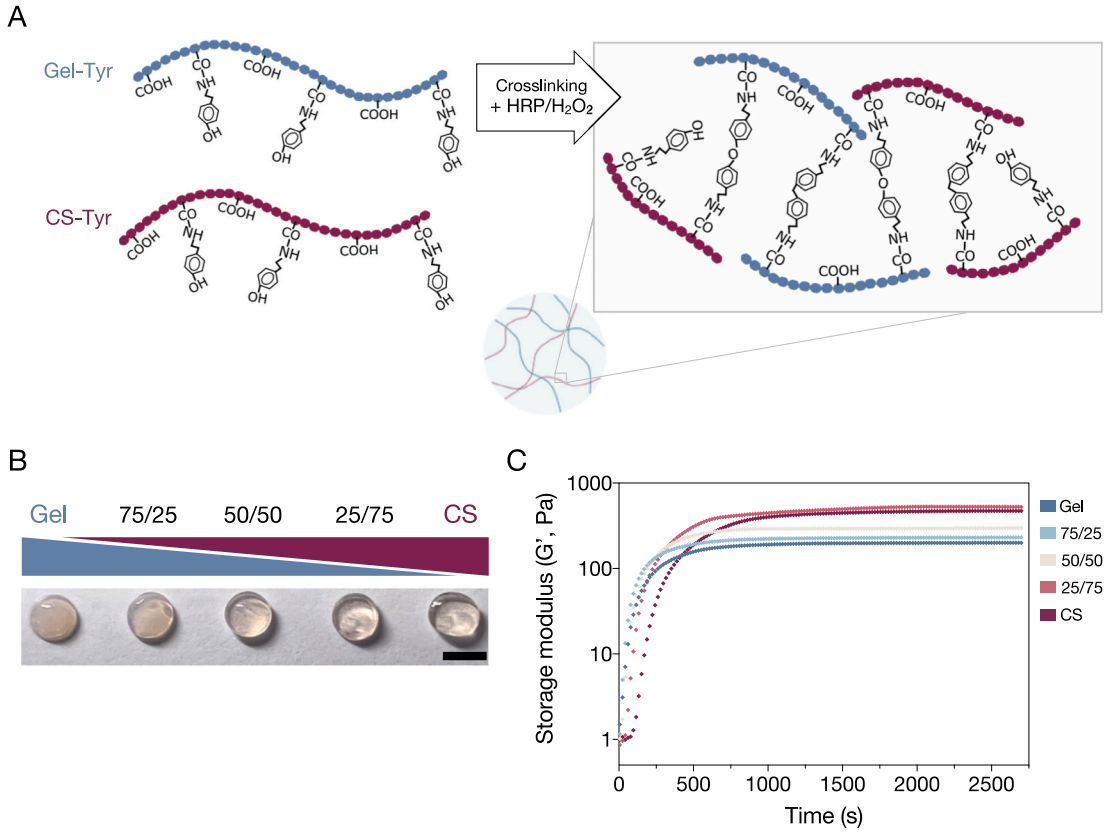

Fig. 1. Gel/CS hydrogel synthesis. (A) Scheme of the enzymatic crosslinking reaction by HRP in the presence of H_2O_2 of Gel-Tyr and CS-Tyr, which leads to C—C and C—O bonds among different polymeric chains. (B) Macroscopic images of the different Gel/CS (4 %, *w/v*) mixtures in the F12 medium with a final concentration of 1.25 U/mL HRP and 2 mM H_2O_2. Scale bar = 0.5 cm. (C) Gelation kinetics through a time sweep of the storage modulus at a strain of 1 % and a frequency of 1 Hz for calculating gelation times.

Table 1
Physico-chemical properties of the Gel/CS hydrogels.

	Gel	75/25	50/50	25/75	CS
Gelation time (min)	1.8 ± 0.5	1.6 ± 0.4	1.7 ± 0.3	3.4 ± 0.7*#$	4.7 ± 0.5*#$^
Pore size (μm)	8 ± 2	12 ± 3*	14 ± 3*#	25 ± 6*#$	59 ± 19*#$^
T_g (°C)	−65	−68	−63	−59	−70
EWC RH 75 % (%)	53.6 ± 5.6	51.4 ± 3.3	51.6 ± 4.1	41.4 ± 3.4*#$	41.5 ± 6.9*#$
EWC relax state (%)	31.7 ± 2.2	30.8 ± 1.9	32.6 ± 4.2	27.3 ± 1.9	26.4 ± 4.5
EWC swollen state (%)	20.1 ± 1.5	25.8 ± 1.0	41.1 ± 2.0*#	56.0 ± 0.5*#$	77.9 ± 9.4*#$^
Crosslinking density (mol/m^3)	46.3 ± 7.4	50.5 ± 5.9	32.7 ± 2.9*#	22.9 ± 2.0*#$	16.3 ± 2.7*#$
Theoretical G' (kPa) dry hydrogels	5.5 ± 0.5	5.3 ± 1.0	4.5 ± 0.7	2.2 ± 0.3*#$	1.6 ± 0.4*#$

*At least $p < 0.005$ (compared to Gel); #at least $p < 0.005$ (compared to 75/25); $at least $p < 0.005$ (compared to 50/50); ^ at least $p < 0.005$ (compared to 25/75); ($n = 3$; ANOVA test followed by Tukey's multiple comparison test). EWC: equilibrium water content.

75 % relative humidity for 7 days. All the hydrogels showed a single glass transition temperature (T_g), which supports the non-phase separation between components. The different T_g values for all the hydrogels appear in Table 1, along with the water retention capacity in this specific assay. There were no significant differences among hydrogels, with the T_g of mixtures falling within the range of the pure ones.

3.2. Influence of CS content of hydrogels on mechanical properties and water retention

The mechanical properties of all the hydrogel mixtures were determined under two different conditions: in what has been described as the relaxed state (after gelation with aqueous solution) [23] and swollen (after immersion for 24 h in culture media). The G' values of the two different states presented opposite tendencies depending on CS content (Fig. 3A). For the relaxed state, G' rose as CS content increased. The swollen Gel had a G' of 137 Pa, similarly to the relaxed one. However as CS content increased, the mechanical properties decreased to a G' value of 57 Pa for the swollen CS. G'' had values within the 2–7 Pa range for all the mixtures (Fig. 3B). The comparison of both values (G' and G'') revealed the elastic behaviour of hydrogels given that $G' \gg G''$. The mechanical properties of the dry hydrogels (Table 1) determined having to use the rubber elasticity theory [23], which gave higher values than the hydrated hydrogels, but displayed the same trend. After gelation,

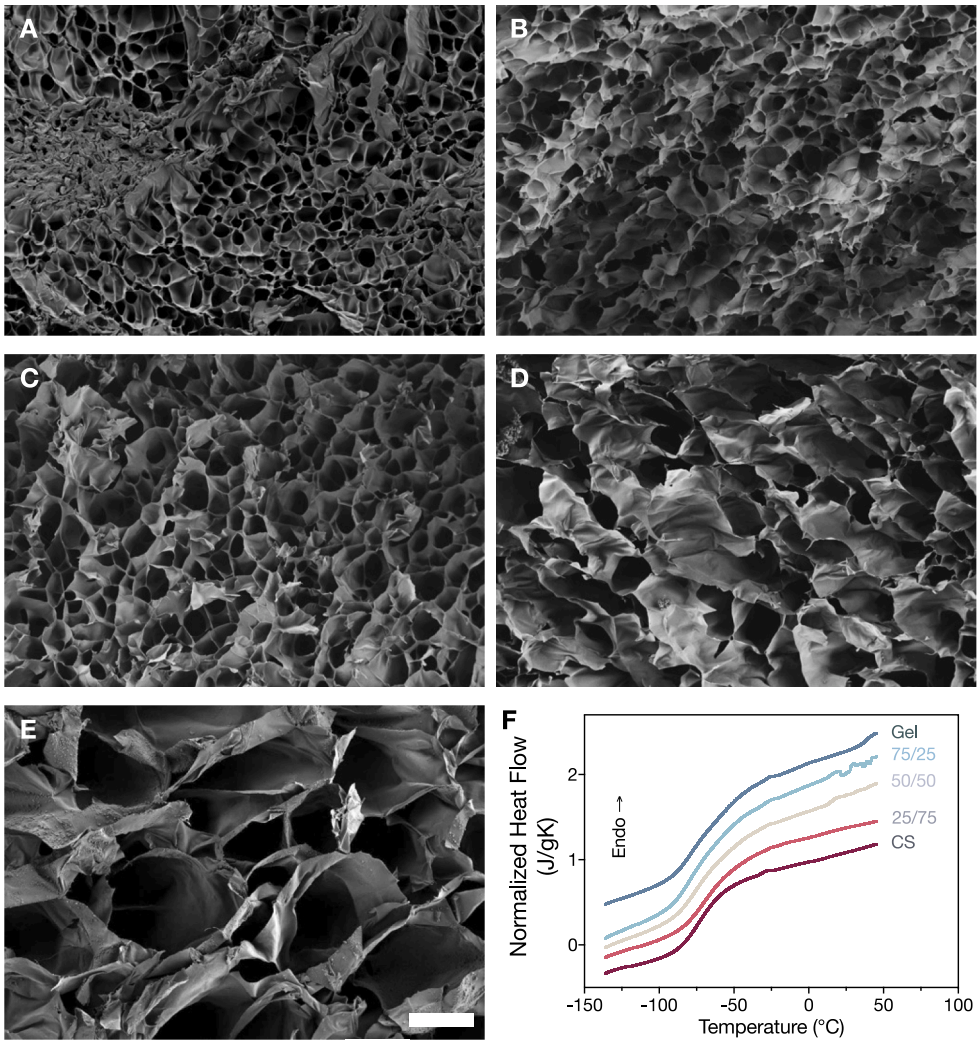

Fig. 2. Morphology and thermal behaviour of the Gel/CS hydrogels. Field emission scanning electron microscope (FE-SEM) images of the lyophilised Gel/CS hydrogels of different compositions (A) Gel (B) 75/25 (C) 50/50 (D) 25/75 and (E) CS. Scale bar (20 μm) applies to all the images. (F) Differential calorimetry scans (2nd heating) at 75 % relative humidity of the Gel/CS hydrogels.

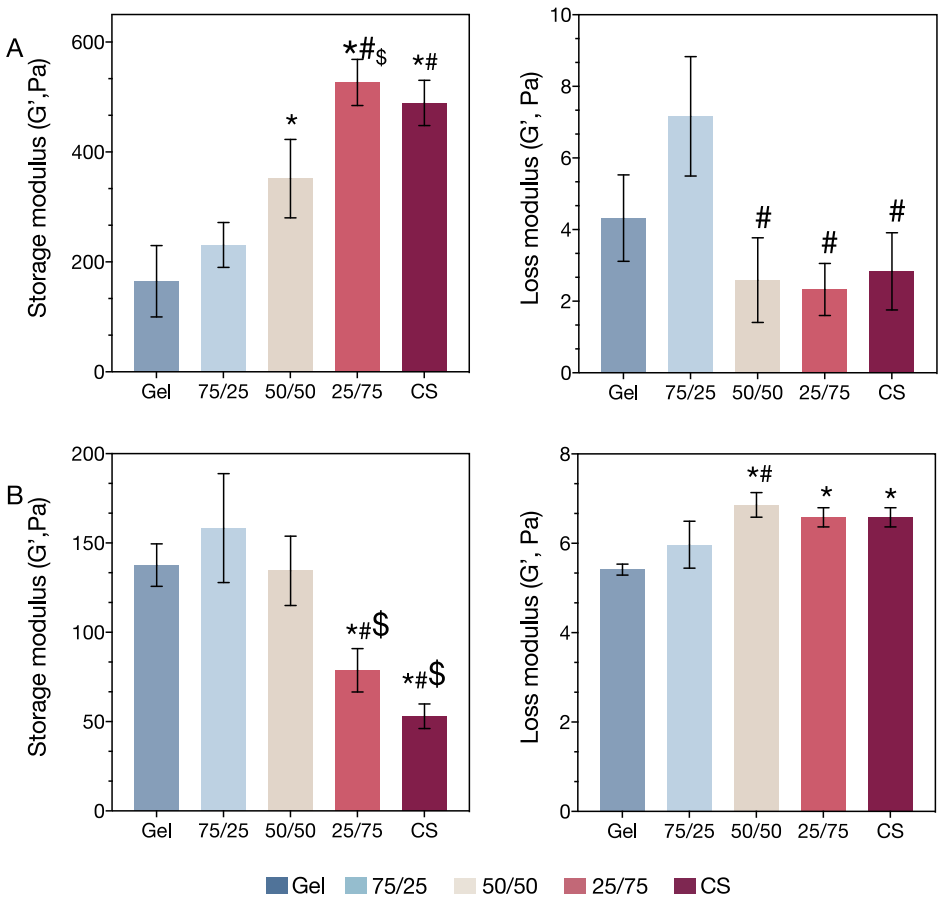

Fig. 3. Rheological characterisation of the Gel/CS hydrogels at a strain of 1 % and a frequency of 1 Hz. (A) Experimental storage modulus and loss modulus in the relaxed state (B) and in the swollen state after 24 h in culture medium. *At least $p < 0.005$ (compared to Gel); #at least $p < 0.005$ (compared to 75/25); $at least $p < 0.005$ (compared to 50/50); ($n = 3$; parametric Student's *t*-test).

hydrogels presented similar water retention capacity. Nonetheless once swollen, the quantity of water increased with CS content, probably due to the lower crosslinking density of CS (Table 1) and the higher affinity of CS for water than Gel (lower Flory-Huggins parameter value than Gel) [15,30].

3.3. Cells encapsulated in the Gel/CS hydrogels survived and expressed key hepatic markers

In order to test the suitability of the developed hydrogels for hepatic cell culture, viability was assessed. No significant differences were found after 1 and 3 days, whereas viability in the 75/25 and 50/50 compositions significantly decreased after 5 culture days (Fig. 4). Despite this reduction, viability always remained above 85 %. Representative images of the live/dead results are presented in Supplementary Fig. S2. To further explore the proliferative activity of the cells cultured in hydrogels, the expression of proliferative marker Ki-67 was analysed by immunofluorescence. It revealed that cells remained proliferative under any condition, even after 5 culture days (Supp. Fig. S3).

The expression of the typical hepatic markers was also assessed by immunofluorescence. The HepG2 cells cultured in the different Gel/CS compositions still showed the expression of A1AT and HNF4 after 5 culture days, grew in clusters and maintained cell-cell contact (Fig. 4B).

3.4. Cells encapsulated in the Gel/CS hydrogels showed increased hepatic functionality

The presence of the mRNA encoding for the key proteins produced by hepatocytes (*i.e.* albumin, CYP3A4) was then evaluated and the levels of the expression in the different culture systems were comparatively analysed during the culture period (1, 3 and 5 days) (Fig. 5A). Quantitative PCR revealed that the HepG2 cells cultured in the Gel/CS hydrogels expressed the genes that were associated with hepatic functions, such as *ALB*. After 3 and 5 culture days, *ALB* expression was higher in the proposed hydrogels than in the monolayer cultures, which may indicate an advantage of the Gel/CS hydrogels for hepatic cell culture. Moreover, given that liver metabolism encompasses a wide range of key processes that maintain homeostasis, the genes encoding for phase I and II enzymes, as well as the MRP2 transporter, were comparatively studied. Although CYP3A4 expression only increased slightly after 5 culture days, phase II enzymes, such as *UGT1A1*, *BAAT* or *GSTA1*, increased in the Gel/CS hydrogels after 3 culture days. *MRP2* expression increased in our 3D systems after 3 culture days, but this increase only remained after 5 days in the Gel hydrogels. The analysis also showed overexpression of *ITGB1* or *CTNNB1* (cell-matrix and cell-cell interaction markers, respectively) in the cells encapsulated in the Gel/CS hydrogels.

Functional assays were also performed to further characterise our 3D cultures. Regarding urea production, after 1 day the cells in the CS compositions (75/25 and 50/50) significantly increased compared to the cells cultured in Gel, and the 50/50 composition obtained the best results. At day 3, the cells in 50/50 exhibited significantly decreased production compared to those embedded in Matrigel®. Nevertheless, the cells in 50/50 increased urea production by day 5, which was significantly higher than in the 75/25 composition (Fig. 5B).

HepG2 cells secreted high albumin levels in culture media, with higher levels detected in the cells cultured in the Gel/CS hydrogels after 5 days compared to the monolayer cultures or the cells encapsulated in Matrigel®, which is consistent with the transcriptomic data (Fig. 5C).

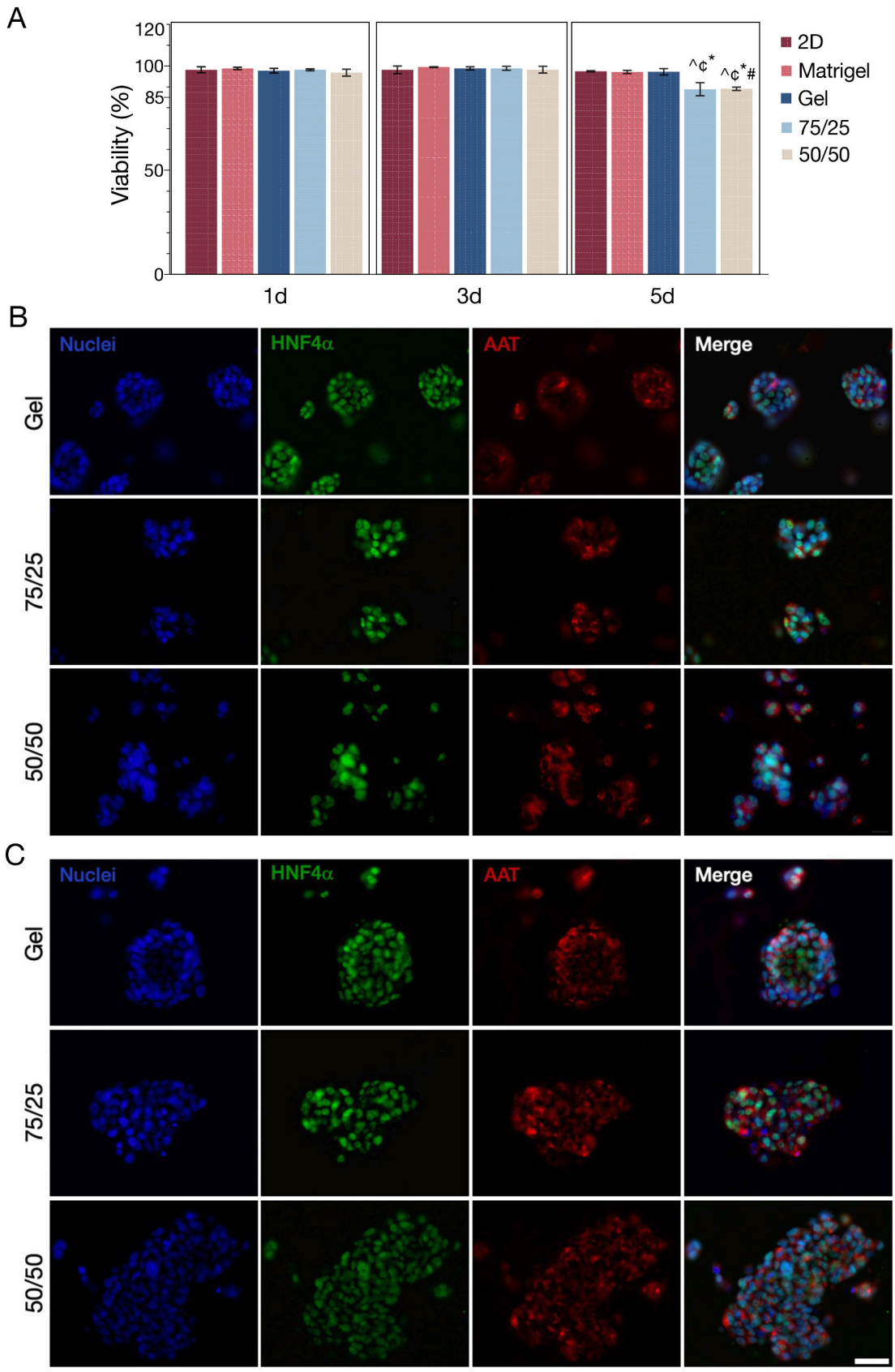

Fig. 4. Characterisation of the HepG2 cells encapsulated in the Gel/CS hydrogels. (A) Cell viability quantification after 1, 3 and 5 culture days (n = 3). ^At least $p < 0.05$ (compared to 2D); $^{¢}p < 0.05$ (compared to Matrigel®); $^{*}p < 0.05$ (compared to Gel); $^{\#}p < 0.05$ (compared to 75/25); (n = 3; ANOVA followed by Tukey's multiple comparison test). (B) Representative confocal immunofluorescence images of the A1AT expression (Green) and HNF4α (Red) after 3 and (C) 5 days. Nuclei were identified by Hoechst 33342 staining (Blue). Scale bar (40 μm) applies to all the images.

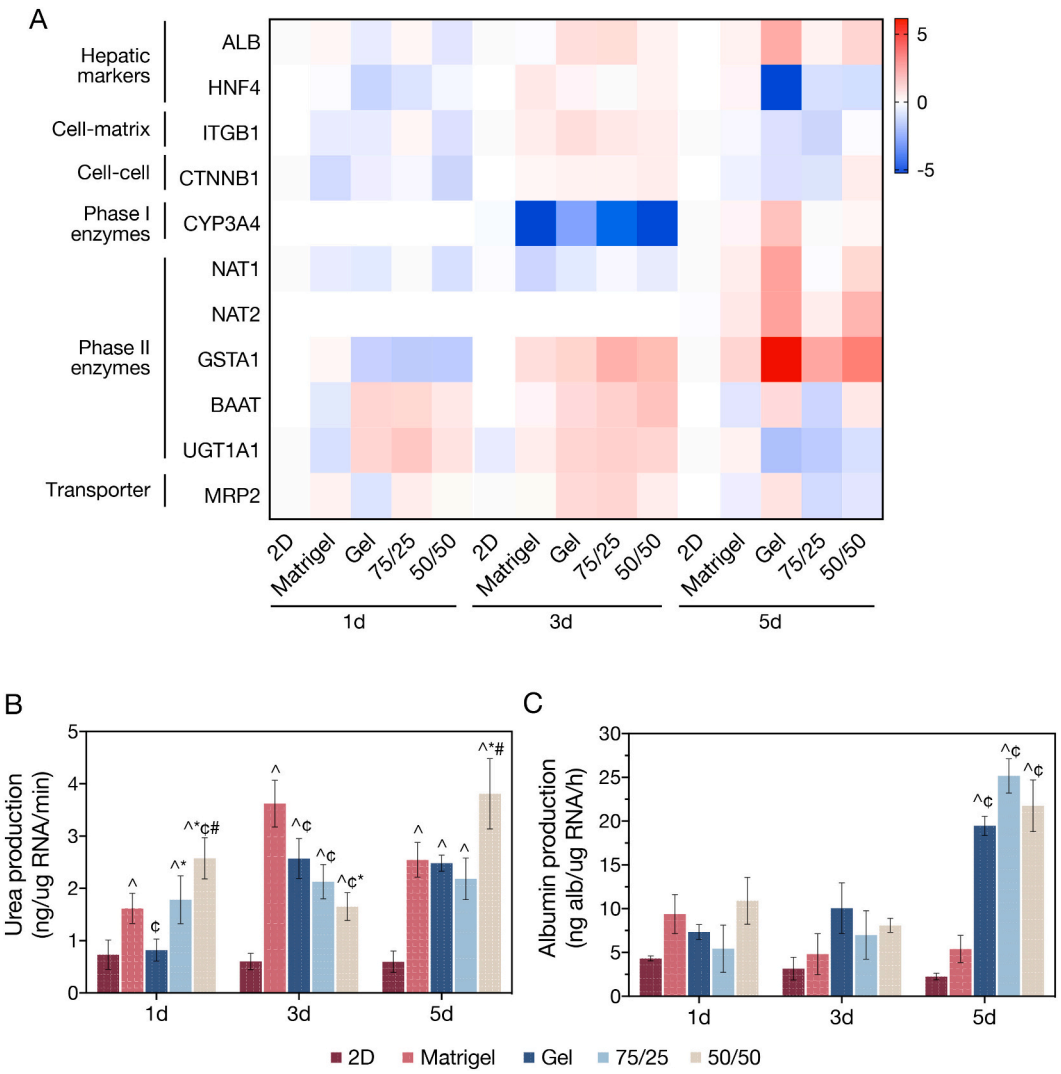

Fig. 5. Transcriptomic and functional characterisation of the HepG2 cells encapsulated in Matrigel® and the Gel/CS hydrogels (Gel, 75/25 and 50/50) after 1, 3 and 5 culture days. (A) The relative gene expression results are represented as the mean of fold change and were normalised by housekeeping genes ($n = 4$). Non-detected samples are represented in white. (B) Urea production is expressed as ng/ug RNA/min (n = 4). (C) Albumin production is expressed as ng/ug RNA/h ($n = 2$) ^At least $p < 0.05$ (compared to 2D); ¢$p < 0.05$ (compared to Matrigel®); *$p < 0.01$ (compared to Gel); #$p < 0.05$ (compared to 75/25); (ANOVA followed by Tukey's multiple comparison test).

4. Discussion

3D-dimensional hydrogel-based liver *in vitro* platforms can be used for drug screening or disease modelling applications if they demonstrate being more physiologically relevant or improve the metabolic performance of cells. For this reason, considering that the proper characterisation of the developed 3D systems from the mechanical and biological points of view is key for the accurate translation and use of these new systems, we fully characterised our Gel/CS hydrogel *in vitro* system to show its suitability for hepatology studies. In this article, we characterised a new hydrogel-based system for hepatic cells culture by proving their suitability for improving the metabolic performance of cells.

The gelation times for the Gel/CS mixtures fell within the range of the rapid gelation process by preventing cell migration or deposition outside the hydrogel. The prolonged gelation time trend according to CS content can be explained by unfavourable interactions with the active site of HRP caused by the bigger number of acidic groups in CS chains (*e.g.*, $—OSO_3^-$ and $—COO^-$) due to either steric hindrance or charge interactions [29]. Despite the different gelation times among hydrogels, the homogenous mixtures without separated domains rich in one of the two polymers were achieved. This means that the cultured cells in mixtures would interact with both molecules Gel and CS.

Understanding the mechanical properties of human liver tissue is a key factor for the development of reliable liver *in vitro* platforms [13]. Although different techniques have been used for determining liver mechanical properties [31,32], the measurement by transient elastography *in vivo* using a healthy human liver has shown a shear modulus ranging from 0.8 to 2.3 kPa at 50 Hz [33,34]. We measured all the compositions to determine, for the first time, the range of mechanical values that Gel/CS can deliver. We selected that which exhibited liver-like behaviour. The rheological properties in the relaxed state of the CS-enriched hydrogels fell within the range of human liver storage modulus values and were comparable to the Gel-based hydrogels [15,27]. Finally, the Gel-enriched compositions were selected for the cell culture because they obtained the highest G' values in the swollen state.

The CS-enriched hydrogels presented higher water absorption capability, possibly for two main reasons: (*i*) the hydrophilic characteristic of CS (the presence of sulphate and carboxylic groups in its backbone, which allow more hydrogen bonds with water molecules) and (*ii*) lower crosslinking density. Although CS presented higher Tyr grafting than Gel, which should give rise to higher crosslinking density,

our data demonstrate the opposite and the CS-enriched hydrogels presented lower crosslinking density than Gel. This finding might be attributed to steric hindrance during the crosslinking reaction provided by the glycosaminoglycan molecules of CS compared to the amino acids of Gel. Despite CS not providing any hydrogels reinforcement in the swollen state (due to good water retention ability), its incorporation was expected to promote some effect on cell behaviour for being a component of the hepatic ECM. Thus while the CS-enriched hydrogels exhibited good water retention, mechanical properties drastically decreased, and moved away from the values obtained for native tissue. This limitation can be solved by modifying polymeric structures and generating a second crosslinking [35].

To determine the functionality and biocompatibility of the 3D Gel-CS hydrogels, the viability and proliferation of the HepG2 cells were monitored for a period lasting up to 5 days. Several authors have demonstrated the non-cytotoxicity of the enzymatic crosslinking used in this study for different materials: Gel, hyaluronic acid and CS [28,29]. Cells remained viable and proliferative for up to 5 days under all the studied conditions, which would allow them to be used for different applications. These results agree with other reports showing positive effects of CS on hepatocyte viability employing an *in vivo* model [36].

Additionally, confocal microscopy images highlighted the non-flattened cell morphology and how cells grew in 3D clusters when in contact with one another and when wholly embedded in hydrogel. This situation came closer to *in vivo* conditions and allowed cells to establish a 3D interconnected network with cell-cell and cell-matrix communications. These results fall in line with the expression analysis of *ITGB1* and *CTNNB1*. *ITGB1* is a basal membrane marker that allows the cell-ECM interaction, while *CTNNB1* is known to localise mainly at lateral junctions and promotes cell-cell interactions. The cells encapsulated in the Gel/CS hydrogels showed an overexpression of both genes on day 3, and was maintained in the 50/50 composition. The simultaneous expression of both markers indicates basal-lateral polarisation in the encapsulated HepG2 spheroids [14,37,38]. Establishing an accurate microstructure is essential for liver function [39]. In fact, cell polarisation has been shown to enhance liver-specific functions, such as urea and albumin production, as well as the expression of metabolic enzymes [38]. This implies that integrins play a key role in hepatocyte-ECM interactions and impact both liver function and regeneration [40].

One of the major functions of hepatocytes is the metabolism of different substances, including drugs, endogenous compounds and xenobiotics, through two different phases: phase I and phase II [1,4]. Phase I is primarily mediated by CYP enzymes, whereas phase II metabolism is mediated by various enzymes, including UGT, SULT and GST. The transcriptomic analysis of the HepG2 cultured in different Gel/CS hydrogels revealed the regulation of the genes encoding for phase I (CYP3A4) and phase II (GSTA1, BAAT, UGT1A1) enzymes after 3 culture days. Despite the limitations of HepG2 in terms of the very low expression levels of phase I and phase II enzymes, or even being non-detectable, our research showed the overexpression of the genes encoding for relevant enzymes implicated in drug metabolism. Based on the results, our 3D systems come closer to *in vivo* than the 2D culture, and can be considered a potential *in vitro* system for drug screening.

Besides metabolic activity, urea and albumin production are considered key hepatic markers to be assessed in the development of liver *in vitro* models as cell performance indicators [3,41,42]. In our hydrogels, the 3D encapsulated cells exhibited greater albumin and urea production than the 2D cultures. In our systems this indicates that cells' functionality improves. In particular, the cells encapsulated in the 50/50 composition had the highest albumin and secretion levels, even compared to Matrigel®, which implies the positive effect of CS. These results are supported by *ALB* expression up-regulation at 3 culture days in hydrogels, which was maintained for up to 5 days in the 50/50 composition.

To our knowledge, this is one of the first studies to explore the effect of CS on the behaviour of liver cells. Despite being a material present in the hepatic matrix, it has not been extensively explored in other 3D models. Although our results illustrate a positive effect on HepG2 cells' performance, further testing of the potential application to assess drug-induced toxicity is necessary for its use as a cell-based drug screening model.

5. Conclusions

In this study, we characterise a novel liver *in vitro* platform based on enzymatically crosslinked Gel/CS hydrogels. These hydrogels exhibit rapid gelation, homogeneous polymer distribution and shear storage moduli within the range of human liver tissue, with CS content positively correlating with mechanical strength. Incorporating CS enhances the water absorption of hydrogels, which results in a reduction of the storage modulus after swelling. Gel-enriched compositions were selected for studying biological response and behaviour because they exhibit liver-like properties after swelling. Our platform shows increased functionality of HepG2 cells (*i.e.* increased ureogenic capacity and albumin secretion) compared to monolayer cultures, which could result in more predictive platforms. Extensive characterisation, which includes not only viability, but also key hepatic functionalities, as well as transcriptomic characterisation, provide increased knowledge of the 3D culture of HepG2 cells, which can support the future translation of these new cell models to preclinical settings. The increased expression of the phase I and phase II enzymes in the cells cultured in the Gel/CS hydrogels suggests that this system could be useful for hepatotoxicity detection by offering more predictive tools than traditional monolayer cultures, especially for detecting compounds that require metabolisation. So the next steps will include the evaluation of the developed platforms as screening tools in the drug development process, although other applications, such as disease modelling, could also be tested.

Abbreviations

CS	chondroitin sulphate
CYP	cytochrome
ECM	extracellular matrix
EWC	equilibrium water content
Gel	gelatin
HRP	Horseradish peroxide
T_g	glass transition temperature
Tyr	tyramine
2D	two-dimensional
3D	three-dimensional

CRediT authorship contribution statement

E. Sanchez-Gonzalez: Writing – original draft, Methodology. **R. Naranjo-Alcazar:** Writing – original draft, Methodology. **I. Tort-Ausina:** Methodology. **M.T. Donato:** Writing – review & editing, Funding acquisition. **M. Salmeron-Sanchez:** Writing – review & editing, Supervision, Formal analysis, Conceptualization. **L. Tolosa:** Writing – review & editing, Writing – original draft, Supervision, Funding acquisition, Formal analysis, Conceptualization. **G. Gallego-Ferrer:** Writing – review & editing, Writing – original draft, Supervision, Funding acquisition, Formal analysis, Conceptualization.

Funding

This study has been supported by the Institute of Health Carlos III and co-financed by the European Union through Grant PI21/00223, and by the Spanish Ministry of Science and Innovation MCIN/AEI/10.13039/501100011033 by PID2022-136433OB-C21, PID2022-136433OB-C22 and CNS2022-135425 grants. This study has also been supported by the Generalitat Valenciana through Grant No. ACIF/2021/378 awarded to E.S.G., and by the Spanish Ministry of Science and Innovation through

Grant PRE2020-094368 awarded to R.N.A.

Declaration of competing interest

The authors declare that they have no known competing financial interests or personal relationships that could have appeared to influence the work reported in this paper. The funders played no role in the design of the study, the collection, analyses, or interpretation of data, in writing the manuscript or in the decision to publish the results.

Acknowledgements

The authors are grateful for the technical support from the Microscopy Service of the Universitat Politècnica de València. The technical assistance of N. Jiménez and A. Gómez is acknowledged.

Appendix A. Supplementary data

Supplementary data to this article can be found online at https://doi.org/10.1016/j.ijbiomac.2024.138693.

Data availability

The raw/processed data required to reproduce these findings cannot be shared at this time due to technical and time limitations. Data will be made available upon reasonable request.

References

[1] P. Godoy, N.J. Hewitt, U. Albrecht, M.E. Andersen, N. Ansari, S. Bhattacharya, J. G. Bode, J. Bolleyn, C. Borner, J. Böttger, A. Braeuning, R.A. Budinsky, B. Burkhardt, N.R. Cameron, G. Camussi, C.S. Cho, Y.J. Choi, J. Craig Rowlands, U. Dahmen, G. Damm, O. Dirsch, M.T. Donato, J. Dong, S. Dooley, D. Drasdo, R. Eakins, K.S. Ferreira, V. Fonsato, J. Fraczek, R. Gebhardt, A. Gibson, M. Glanemann, C.E.P. Goldring, M.J. Gómez-Lechón, G.M.M. Groothuis, L. Gustavsson, C. Guyot, D. Hallifax, S. Hammad, A. Hayward, D. Häussinger, C. Hellerbrand, P. Hewitt, S. Hoehme, H.G. Holzhütter, J.B. Houston, J. Hrach, K. Ito, H. Jaeschke, V. Keitel, J.M. Kelm, B. Kevin Park, C. Kordes, G.A. Kullak-Ublick, E.L. Lecluyse, P. Lu, J. Luebke-Wheeler, A. Lutz, D.J. Maltman, M. Matz-Soja, P. McMullen, I. Merfort, S. Messner, C. Meyer, J. Mwinyi, D.J. Naisbitt, A. K. Nussler, P. Olinga, F. Pampaloni, J. Pi, L. Pluta, S.A. Przyborski, A. Ramachandran, V. Rogiers, C. Rowe, C. Schelcher, K. Schmich, M. Schwarz, B. Singh, E.H.K. Stelzer, B. Stieger, R. Stöber, Y. Sugiyama, C. Tetta, W.E. Thasler, T. Vanhaecke, M. Vinken, T.S. Weiss, A. Widera, C.G. Woods, J.J. Xu, K. M. Yarborough, J.G. Hengstler, Recent advances in 2D and 3D in vitro systems using primary hepatocytes, alternative hepatocyte sources and non-parenchymal liver cells and their use in investigating mechanisms of hepatotoxicity, cell signaling and ADME, Arch. Toxicol. 87 (2013) 1315–1530, https://doi.org/10.1007/s00204-013-1078-5.

[2] I. Allu, A.K. Sahi, M. Koppadi, S. Gundu, A. Sionkowska, Decellularization techniques for tissue engineering: towards replicating native extracellular matrix architecture in liver regeneration, J. Funct. Biomater. 14 (2023) 518, https://doi.org/10.3390/jfb14100518.

[3] M.J. Gómez-Lechón, L. Tolosa, I. Conde, M.T. Donato, Competency of different cell models to predict human hepatotoxic drugs, Expert Opin. Drug Metab. Toxicol. 10 (2014) 1553–1568, https://doi.org/10.1517/17425255.2014.967680.

[4] F. Bonanini, M. Singh, H. Yang, D. Kurek, A.C. Harms, A. Mardinoglu, T. Hankemeier, A comparison between different human hepatocyte models reveals profound differences in net glucose production, lipid composition and metabolism in vitro, Exp. Cell Res. 437 (2024) 114008, https://doi.org/10.1016/j.yexcr.2024.114008.

[5] C.C. Bell, D.F.G. Hendriks, S.M.L. Moro, E. Ellis, J. Walsh, A. Renblom, L. Fredriksson Puigvert, A.C.A. Dankers, F. Jacobs, J. Snoeys, R.L. Sison-Young, R. E. Jenkins, Å. Nordling, S. Mkrtchian, B.K. Park, N.R. Kitteringham, C.E. P. Goldring, V.M. Lauschke, M. Ingelman-Sundberg, Characterization of primary human hepatocyte spheroids as a model system for drug-induced liver injury, liver function and disease, Sci. Rep. 6 (2016) 25187, https://doi.org/10.1038/srep25187.

[6] A. Vasudevan, N. Majumder, I. Sharma, I. Kaur, S. Sundarrajan, J.R. Venugopal, P. Vijayaraghavan, N. Singh, S. Ramakrishna, S. Ghosh, D.M. Tripathi, S. Kaur, Liver extracellular matrix-based nanofiber scaffolds for the culture of primary hepatocytes and drug screening, ACS Biomater Sci. Eng. 9 (2023) 6357–6368, https://doi.org/10.1021/acsbiomaterials.3c01216.

[7] S. Ye, J.W.B. Boeter, L.C. Penning, B. Spee, K. Schneeberger, Hydrogels for liver tissue engineering, Bioengineering 6 (2019) 59, https://doi.org/10.3390/bioengineering6030059.

[8] L.A. Milton, J.W. Davern, L. Hipwood, J.D.S. Chaves, J. McGovern, D. Broszczak, D. W. Hutmacher, C. Meinert, Y.C. Toh, Liver click dECM hydrogels for engineering hepatic microenvironments, Acta Biomater. 185 (2024) 144–160, https://doi.org/10.1016/j.actbio.2024.06.037.

[9] Z. Jiang, B. Jin, Z. Liang, Y. Wang, S. Ren, Y. Huang, C. Li, H. Sun, Y. Li, L. Liu, N. Li, J. Wang, Z. Cui, P. Huang, H. Yang, Y. Mao, H. Ye, Liver bioprinting within a novel support medium with functionalized spheroids, hepatic vein structures, and enhanced post-transplantation vascularization, Biomaterials 311 (2024) 122681, https://doi.org/10.1016/j.biomaterials.2024.122681.

[10] R. Rajalekshmi, A. Kaladevi Shaji, R. Joseph, A. Bhatt, Scaffold for liver tissue engineering: exploring the potential of fibrin incorporated alginate dialdehyde–gelatin hydrogel, Int. J. Biol. Macromol. 166 (2021) 999–1008, https://doi.org/10.1016/j.ijbiomac.2020.10.256.

[11] A.B. Bello, D. Kim, D. Kim, H. Park, S.H. Lee, Engineering and functionalization of gelatin biomaterials: from cell culture to medical applications, Tissue Eng. Part B Rev. 26 (2020) 164–180, https://doi.org/10.1089/ten.teb.2019.0256.

[12] L. Di Muzio, C. Sergi, V.C. Carriero, J. Tirillò, A. Adrover, E. Messina, R. Gaetani, S. Petralito, M.A. Casadei, P. Paolicelli, Gelatin-based spongy and compressive resistant cryogels with shape recovery ability as ideal scaffolds to support cell adhesion for tissue regeneration, React. Funct. Polym. 189 (2023) 105607, https://doi.org/10.1016/j.reactfunctpolym.2023.105607.

[13] N. Carpentier, S. Ye, M.D. Delemarre, L. Van der Meeren, A.G. Skirtach, L.J.W. van der Laan, K. Schneeberger, B. Spee, P. Dubruel, S. Van Vlierberghe, Gelatin-based hybrid hydrogels as matrices for organoid culture, Biomacromolecules 25 (2024) 590–604, https://doi.org/10.1021/acs.biomac.2c01496.

[14] S.Y. Park, W.G. Koh, H.J. Lee, Enhanced hepatotoxicity assessment through encapsulated HepG2 spheroids in gelatin hydrogel matrices: bridging the gap from 2D to 3D culture, Eur. J. Pharm. Biopharm. 202 (2024) 114417, https://doi.org/10.1016/j.ejpb.2024.114417.

[15] J. Rodriguez-Fernandez, E. Garcia-Legler, E. Villanueva-Badenas, M.T. Donato, J. L. Gomez-Ribelles, M. Salmeron-Sanchez, G. Gallego-Ferrer, L. Tolosa, Primary human hepatocytes-laden scaffolds for the treatment of acute liver failure, Biomaterials Advances 153 (2023) 213576, https://doi.org/10.1016/j.bioadv.2023.213576.

[16] A.D. Theocharis, S.S. Skandalis, C. Gialeli, N.K. Karamanos, Extracellular matrix structure, Adv. Drug Deliv. Rev. 97 (2016) 4–27, https://doi.org/10.1016/j.addr.2015.11.001.

[17] J. Luo, Z. Zhang, Y. Zeng, Y. Dong, L. Ma, Co-encapsulation of collagenase type I and silibinin in chondroitin sulfate coated multilayered nanoparticles for targeted treatment of liver fibrosis, Carbohydr. Polym. 263 (2021) 117964, https://doi.org/10.1016/j.carbpol.2021.117964.

[18] S. Sakai, K. Hirose, K. Taguchi, Y. Ogushi, K. Kawakami, An injectable, in situ enzymatically gellable, gelatin derivative for drug delivery and tissue engineering, Biomaterials 30 (2009) 3371–3377, https://doi.org/10.1016/j.biomaterials.2009.03.030.

[19] Y. Zhang, H. Chen, T. Zhang, Y. Zan, T. Ni, Y. Cao, J. Wang, M. Liu, R. Pei, Injectable hydrogels from enzyme-catalyzed crosslinking as BMSCs-laden scaffold for bone repair and regeneration, Mater. Sci. Eng. C 96 (2019) 841–849, https://doi.org/10.1016/j.msec.2018.12.014.

[20] S. Kripotou, E. Stefanopoulou, M. Culebras-Martínez, R.M. Morales-Román, G. Gallego Ferrer, A. Kyritsis, Water dynamics and thermal properties of tyramine-modified hyaluronic acid - gelatin hydrogels, Polymer 178 (2019) 121598, https://doi.org/10.1016/j.polymer.2019.121598.

[21] E. Sanmartín-Masiá, S. Poveda-Reyes, G. Gallego Ferrer, Extracellular matrix–inspired gelatin/hyaluronic acid injectable hydrogels, Int. J. Polym. Mater. Polym. 66 (2017) 280–288, https://doi.org/10.1080/00914037.2016.1201828.

[22] X. Yang, H. Yang, X. Jiang, B. Yang, K. Zhu, N.C.H. Lai, C. Huang, C. Chang, L. Bian, L. Zhang, Injectable chitin hydrogels with self-healing property and biodegradability as stem cell carriers, Carbohydr. Polym. 256 (2021) 117574, https://doi.org/10.1016/j.carbpol.2020.117574.

[23] N.R. Richbourg, N.A. Peppas, The swollen polymer network hypothesis: quantitative models of hydrogel swelling, stiffness, and solute transport, Prog. Polym. Sci. 105 (2020) 101243, https://doi.org/10.1016/j.progpolymsci.2020.101243.

[24] M. Moya, M. Benet, C. Guzmán, L. Tolosa, C. García-Monzón, E. Pareja, J. V. Castell, R. Jover, Foxa1 reduces lipid accumulation in human hepatocytes and is down-regulated in nonalcoholic fatty liver, PloS One 7 (2012) e30014, https://doi.org/10.1371/journal.pone.0030014.

[25] J. Hellemans, G. Mortier, A. De Paepe, F. Speleman, J. Vandesompele, qBase relative quantification framework and software for management and automated analysis of real-time quantitative PCR data, Genome Biol. 8 (2008) 1–14, https://doi.org/10.1186/gb-2007-8-2-r19.

[26] J. Vandesompele, K. De Preter, Ilip Pattyn, B. Poppe, N. Van Roy, A. De Paepe, Rank Speleman, Accurate normalization of real-time quantitative RT-PCR data by geometric averaging of multiple internal control genes, Genome Biol. 3 (2002) 1–12, https://doi.org/10.1186/gb-2002-3-7-research0034.

[27] S. Poveda-Reyes, V. Moulisova, E. Sanmartín-Masiá, L. Quintanilla-Sierra, M. Salmerón-Sánchez, G.G. Ferrer, Gelatin—hyaluronic acid hydrogels with tuned stiffness to counterbalance cellular forces and promote cell differentiation, Macromol. Biosci. (2016) 1311–1324, https://doi.org/10.1002/mabi.201500469.

[28] T.T. Nguyen, L.H. Dang, P. Nguyen, T.L.B. Pham, H.K. Le, M.T. Nguyen, T.T.Y. Nhi, S. Feng, J. Chen, N.Q. Tran, Dual composition chondroitin sulfate and gelatin biomimetic hydrogel based on tyramine crosslinking for tissue regenerative medicine, Eur. Polym. J. 189 (2023) 111975, https://doi.org/10.1016/j.eurpolymj.2023.111975.

[29] F. Chen, S. Yu, B. Liu, Y. Ni, C. Yu, Y. Su, X. Zhu, X. Yu, Y. Zhou, D. Yan, An injectable enzymatically crosslinked carboxymethylated pullulan/chondroitin sulfate hydrogel for cartilage tissue engineering, Sci. Rep. 6 (2016) 1–13, https://doi.org/10.1038/srep20014.
[30] T. Walimbe, A. Panitch, Best of both hydrogel worlds: harnessing bioactivity and tunability by incorporating glycosaminoglycans in collagen hydrogels, Bioengineering 7 (2020) 1–24, https://doi.org/10.3390/bioengineering7040156.
[31] S. Chatelin, J. Oudry, N. Périchon, L. Sandrin, P. Allemann, L. Soler, R. Willinger, In vivo liver tissue mechanical properties by transient elastography: comparison with dynamic mechanical analysis, Biorheology 48 (2011) 75–88, https://doi.org/10.3233/BIR-2011-0584.
[32] Q. Wu, Q. Sun, Q. Zhang, N. Wang, W. Lv, D. Han, Extracellular matrix stiffness-induced mechanotransduction of capillarized liver sinusoidal endothelial cells, Pharmaceuticals 17 (2024) 644, https://doi.org/10.3390/ph17050644.
[33] L. Castera, X. Forns, A. Alberti, Non-invasive evaluation of liver fibrosis using transient elastography, J. Hepatol. 48 (2008) 835–847, https://doi.org/10.1016/j.jhep.2008.02.008.
[34] M. Fraquelli, C. Rigamonti, G. Casazza, D. Conte, M.F. Donato, G. Ronchi, M. Colombo, Reproducibility of transient elastography in the evaluation of liver fibrosis in patients with chronic liver disease, Gut 56 (2007) 968–973, https://doi.org/10.1136/gut.2006.111302.
[35] Z. Geng, Y. Ji, S. Yu, Q. Liu, Z. Zhou, C. Guo, D. Lu, D. Pei, Preparation and characterization of a dual cross-linking injectable hydrogel based on sodium alginate and chitosan quaternary ammonium salt, Carbohydr. Res. 507 (2021) 108389, https://doi.org/10.1016/j.carres.2021.108389.
[36] P.L.R. Guedes, C.P.F. Carvalho, A.A.F. Carbonel, M.J. Simões, M.Y. Icimoto, J.A. K. Aguiar, M. Kouyoumdjian, M.L. Gazarini, M.R. Nagaoka, Chondroitin sulfate protects the liver in an experimental model of extra-hepatic cholestasis induced by common bile duct ligation, Molecules 27 (2022) 1–16, https://doi.org/10.3390/molecules27030654.
[37] S.C. Ramaiahgari, M.W. Den Braver, B. Herpers, V. Terpstra, J.N.M. Commandeur, B. Van De Water, L.S. Price, A 3D in vitro model of differentiated HepG2 cell spheroids with improved liver-like properties for repeated dose high-throughput toxicity studies, Arch. Toxicol. 88 (2014) 1083–1095, https://doi.org/10.1007/s00204-014-1215-9.
[38] M.K. Kim, W. Jeong, S. Jeon, H.W. Kang, 3D bioprinting of dECM-incorporated hepatocyte spheroid for simultaneous promotion of cell-cell and -ECM interactions, Front. Bioeng. Biotechnol. 11 (2023) 1305023, https://doi.org/10.3389/fbioe.2023.1305023.
[39] R. Masuzaki, K.C. Ray, J. Roland, R. Zent, Y.A. Lee, S.J. Karp, Integrin β1 establishes liver microstructure and modulates transforming growth factor β during liver development and regeneration, Am. J. Pathol. 191 (2021) 309–319, https://doi.org/10.1016/j.ajpath.2020.10.011.
[40] S.J.I. Blackford, T.T.L. Yu, M.D.A. Norman, A.M. Syanda, M. Manolakakis, D. Lachowski, Z. Yan, Y. Guo, E. Garitta, F. Riccio, G.M. Jowett, S.S. Ng, S. Vernia, A.E. del Río Hernández, E. Gentleman, S.T. Rashid, RGD density along with substrate stiffness regulate hPSC hepatocyte functionality through YAP signalling, Biomaterials 293 (2023) 121982, https://doi.org/10.1016/j.biomaterials.2022.121982.
[41] M. De Colli, M. Massimi, A. Barbetta, B.L. Di Rosario, S. Nardecchia, L. Conti Devirgiliis, M. Dentini, A biomimetic porous hydrogel of gelatin and glycosaminoglycans cross-linked with transglutaminase and its application in the culture of hepatocytes, Biomed. Mater. (2012) 055005, https://doi.org/10.1088/1748-6041/7/5/055005.
[42] C.Y. Liaw, S. Ji, M. Guvendiren, Engineering 3D hydrogels for personalized in vitro human tissue models, Adv. Healthc. Mater. 7 (2018) 1–16, https://doi.org/10.1002/adhm.201701165.